ILL Number: 67442741

BLC

Shipping Method: Ariel

Yes No Cond

Call #: att

Borrower: UCW

In Process: 20100721

Charge:

Lending String: *MYG,SCW,LYU,NRC,UMC

MaxCost: $75IFM

Patron: Savkar, Amit

Library Address:
Univ of Connecticut
Babbidge Library
DD-ILL Office (U-2005F)
369 Fairfield Way

Journal Title: Reliability, packaging, testing, and characterization of MEMS/MOEMS V ; 25-26 January, 2006, San Jose, California, USA /

Shipping Address:

Volume: 6111 **Issue:**
Month/Year: 2006
Pages: Not sure

Fax: 860-486-3593
Email Address: udoc@uconn.edu

Article Author:

Article Title: Amit A Savkar; Using periodic electrical excitation to achieve stick-release in micro-cantilevers

Request Type: Article
Document Type:

Borrowing Notes: Borrowing Notes; Thank you!

OCLC# 65523225

Imprint: Bellingham, Wash. ; SPIE, c2006.

Ariel Address: 137.99.96.19

Using Periodic Electrical Excitation to Achieve Stick-Release in Micro-Cantilevers

Amit Savkar and Kevin D. Murphy

Department of Mechanical Engineering
University of Connecticut, Storrs, CT 06269-3139, USA

1. ABSTRACT

Recently, it has been proposed that sticking contact between micro-scale components may be relieved (i.e., the components may be unstuck) using structural vibrations. The means to excite these vibrations plays a critical role in the physical mechanism responsible for the initiation of stick-release. For example, it has been shown that mechanical actuation using, say, an instrumented nanoindentor is most effective near a resonant frequency. Aside from showing the fundamental mechanism responsible for the repair (resonance), it also provides insight for choosing optimal excitation parameters, such as excitation amplitude and frequency, for stick-release. In the present paper, periodic electrical excitation is explored as a means of inducing structural vibrations. It is shown that electrical excitation produces stick-release through a fundamentally different mechanism than its mechanical counterpart. Here, stick-release is achieved via unstable self-excited vibrations. This fact has a significant influence on the practical matter of choosing appropriate excitation parameters to produce the desired repair. Using the underlying physics, appropriate parameter combinations are mapped.

2. INTRODUCTION

One critical issue preventing the wide-scale introduction of MEMS into engineered systems is the ongoing problem of long-term reliability. And one common problem is sticking contact, often referred to as stiction failure. This contact may be between neighboring components or between a component and the substrate. For example, Figure 1 shows a schematic of a micro-cantilever (e.g., a comb drive) stuck to the substrate in static equilibrium. Once stiction has been initiated, the stuck beam is no longer free to move as it was intended and the device is said to have failed. There are a variety of forces that may contribute to sticking contact. These include van der Waals forces, micro-capillaries, and electrostatic forces, to name just a few. But regardless of its source, the adhesion energy at the interface is sufficient to prevent the elastic strain energy, created by the deformation in the beam, from restoring the beam to its horizontal, unstuck equilibrium. One approach for improving reliability is to introduce surface treatments that limit the interfacial energy and, therefore, reduce the likelihood of sticking contact. These include hydrogen terminating treatments, self-assembly monolayers, fluorocarbon films, and diamond-like carbon coatings.[1,2] These treatments have successfully reduced the frequency of stiction failures under certain circumstances. Of course, these treatments require additional processing steps, increasing manufacturing time and driving up costs. Moreover, due to geometric constraints, additional material layers may not be an option in some designs.

A second approach to improving reliability is to repair (i.e., unstick) stuck components, such that they may be returned to service. By far the most studied approach involves using short laser pulses, directed at the stuck component.[3–5] The specifics of the release mechanism are not thoroughly understood at the present time, though it has been suggested that either (i) the thermal expansion of the component relative to the substrate leads to relative slip or (ii) thermal buckling drives the component to separate from the substrate.[6] Regardless of the mechanism driving the repair, this strategy has met with considerable success. However, practical implementation of this technique is probably going to be limited to failures that occur during fabrication. Directly after fabrication and before the device is incorporated into a system, the chip may be inspected, mounted in a laser-release apparatus containing all of the necessary optics, and repaired. For components that fail during operation, this is not a realistic option - particularly if the failure is persistent, i.e. if it is re-occurant.

Further author information: (Send correspondence to K. D. Murphy)
e-mail: kdm@engr.uconn.edu, Telephone: +1 860 486 4109

Reliability, Packaging, Testing, and Characterization of MEMS/MOEMS V, edited by Danelle M. Tanner, Rajeshuni Ramesham, Proc. of SPIE Vol. 6111, 611102, (2006) · 0277-786X/06/$15 · doi: 10.1117/12.647841

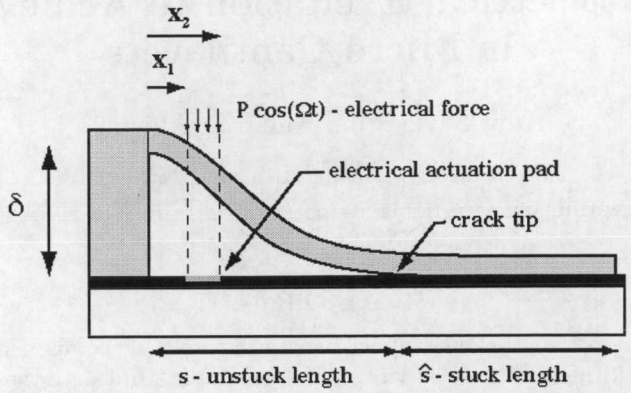

Figure 1: A schematic of a micro-cantilever stuck to a substrate. Its unstuck length is s. A periodic voltage is applied over a small portion of the beam, in an attempt to unstick it.

Recently is has been suggested that structural vibrations might be an effective alternative to laser-pulsed heating for the repair of stiction failed components.[7] The physical process behind this approach can be seen in terms of Figure 1. At the right end of the unstuck section, $x = s$, the beam and the substrate merge and form a singularity, which is geometrically similar to a crack tip. As the unstuck portion of the beam is driven periodically, the crack may or may not advance; the onset of crack propagation (also referred to as peeling, in this physical context) and its continued growth may be described via dynamic fracture mechanics. The preliminary work done focused on determining the excitation parameter combinations of the forcing amplitude and frequency (F, Ω) that *initiated* peeling.[7] There were several key results. At the zero frequency limit, the dynamic force required to initiate peeling asymptotically approached the static peeling force F_s. Near the resonant frequencies, the force required to initiate peeling dropped because of the amplification of the response amplitude. Exceptions to this general rule exist but are rare; these exceptions depend sensitively on the loading geometry and the vibration mode shapes. Lastly, in between resonances, the force required increases dramatically, indicating that a dynamic release process at these parameter combinations is less desirable than near a resonance.

In the present paper, electrical actuation is considered as an alternative to the mechanical loading.[7] Again, consider the schematic of the micro-cantilever shown in Figure 1. If a periodic voltage is applied through an electrical actuation pad on the substrate, a periodic force is exerted on the beam. Specifically, this force is gap-dependent: $f \propto \frac{1}{(\delta - w)^2}$, where $w(x,t)$ is the lateral deflection of the beam. This gap dependent excitation changes the physical mechanism responsible for stick-release. Here, a dynamic instability may initiate the peeling process - as opposed to resonance in the mechanical loading scenario, where the load is gap-independent. This fact may be used to our advantage: a simple stability analysis will clearly identify unstable regions in the voltage - frequency (V, Ω) plane. By driving the system in these regions, the vibration amplitude will grow (without bound, in the linear sense) and promote peeling. This provides a rational for choosing excitation parameters for effective stiction repair.

It should be noted that there are several potential benefits to this electrical vibration repair approach. To begin, the only obvious mechanism for component damage, as a result of the repair process itself, is fatigue. But since most materials have fatigue lives exceeding 10^4 cycles, this won't be an issue even after numerous failure/repair cycles. This stands in marked contrast to thermal repair, where components may warp if too much energy is delivered in any single pulse. Second, electrical excitation is particularly attractive, since it could use the functionality of the chip itself to effect the necessary repair. Moreover, this would permit the repair of components that fail in-operation (i.e., in-service failures) without having to remove the chip from an overall system. Lastly, one may ask about the down side. At first glance, it may appear that vibration repair requires a-priori knowledge of the unstable zones in the (V, Ω) plane. While such calculations are possible for the micro-cantilevers studied here, they are not trivial for the complex component geometries and boundary/contact conditions encountered in real MEMS devices. However, these unstable regions are reasonably large, such that

the excitation frequency may be swept until an instability is encountered and the necessary repair is achieved.

3. THE MATHEMATICAL MODEL

The system under consideration is a stuck micro-cantilever, as shown schematically in Figure 1. These structures were chosen because of their simple geometries, well defined contact areas, and the availability of MEMS cantilevers to be used in future (anticipated) tests.

3.1. The Vibration-Electrical Model

The structural model consists of a uniform, linear elastic beam with net length L, an initial unstuck length s ($L = s + \hat{s}$), a rectangular cross section with thickness h and depth b (cross-sectional area $\bar{A} = bh$), and mass per unit length m. The structural damping is uniform throughout and viscous, with a damping coefficient c. Squeeze-film effects may be relevant, but would be localized near the crack tip. As a rule of thumb, this model is valid for low pressure scenarios and for deformations that do not exceed the beam thickness. The latter is guaranteed if the gap separation is less than the thickness, $\delta < h$. The equation governing the lateral displacement of the beam is simply:

$$m\ddot{W} + c\dot{W} + EIW_{,xxxx} = F(x,t), \tag{1}$$

where W is the lateral deflection, $I = bh^3/12$ is the moment of inertia and dots refer to derivatives with respect to time and $\bullet_{,x} = \partial \bullet / \partial x$ refers to differentiation with respect to space. $F(x,t)$ is the external excitation.

The excitation is provided by a small actuation pad located on the substrate, as shown in Figure 1. The electrical force is applied over a region of the beam between $x_1 < x < x_2$ and is gap dependent. This means that the force delivered is deflection dependent. Specifically, the force is given by:

$$F_e(x,t) = \frac{\epsilon_o \bar{A}}{2} \frac{V^2(t)}{[\delta - W(x,t)]^2} \left[H(x - x_1) - H(x - x_2) \right], \tag{2}$$

where ϵ_o is the permittivity in air, $V(t) = V_o \cos(\Omega t)$ is the periodic voltage, and $H(x - x_i)$ is the Heavyside step function, which steps from zero to one at $x = x_i$.

To simplify matters, Equations (1) and (2) may expressed in nondimensional form. The position along the beam is normalized by the total unstuck length, $\xi = x/s$. This is an appropriate choice because the focus is on the initiation of crack advance, for which s is constant. The lateral deflection is normalized by the gap size $w = W/\delta$. Introducing these quantities into Equations (1) and (2) leads to

$$m\delta\ddot{w} + c\delta\dot{w} + EIw_{,\xi\xi\xi\xi} = \frac{\epsilon_o \bar{A}}{2} \frac{V_o^2 \cos^2(\Omega t)}{[1 - w]^2} \left[H(\xi - \xi_1) - H(\xi - \xi_2) \right]. \tag{3}$$

Provided the actuation pad is located sufficiently close to the post support, the deformation of the loaded portion of the beam is small, i.e. $w << 1$. In this case, the binomial expansion may be used to expand the gap-dependent forcing term:

$$\frac{1}{[1 - w]^2} \approx 1 + 2w + \mathcal{O}(w^2). \tag{4}$$

A nondimensional time, $\tau = 2\Omega t$, and the binomial expansion may be introduced into Equation (3). Using a one mode Galerkin expansion ($w(x,t) = a(t)\Psi(x)$) all spatial dependence is eleminated, leaving an ODE with periodic coefficients:

$$\ddot{A}(\tau) + \mu\dot{A}(\tau) + \left[a + \epsilon + \epsilon\cos(\tau) \right] A(\tau) = \frac{\epsilon \cos(\tau)}{a}. \tag{5}$$

Here $\mu = \zeta/r$, $a = 1/4r^2$, $\epsilon = -\kappa a V_o^2$, and $\kappa = \epsilon_o \bar{A}/\delta^3 k$. Also, $r = \Omega/\omega$ is the normalized excitation frequency. Equation (5) is a version of Mathieu's equation and the parameters μ, a, and ϵ are the Mathieu parameters. This equation is a linear, nonhomogeneous ordinary differential equation with periodic coefficients for the unknown modal amplitudes $A(\tau)$. It is worth noting that any mode shape Ψ_i could be used in the discretization process. For the remainder of this work, the first vibration mode is retained.

It is also worth considering the influence of the initial geometry on the vibration behavior. The stuck beam of Figure 1 is initially deformed and vibrations occur about that deformed state. However, because all of the deformations are linear, superposition applies; the initial deformation and the vibration behavior may be examined separately and then superposed at the end. Of course, since the objective is to promote unstable oscillations (where $A(\tau) \rightarrow \infty$ in this linear model), the initial deformation will be of little consequence. Hence, the focus will remain on the vibration response of a clamped-clamped beam.

3.2. Solution Procedure

The total solution to Equation (5) is the sum of the transient solution, a_t, and steady-state solution, a_{ss}, corresponding to the homogeneous and nonhomogeneous forms of the equation of motion, respectively. Moreover, it is well established that these Mathieu equations may possess unbounded (unstable) homogeneous solutions.[8] In this case, the total solution $a_{\text{total}} = a_t + a_{ss}$ is also unbounded, regardless of the behavior of a_{ss}. The goal is to capitolize on this unbounded response, as it should promote repair. Consequently, the objective is to identify parameter combinations that lead to *periodic* transient solutions, since these solutions serve as a natural demarcation between bounded (decaying) transient solutions and unbounded (growing) transient solutions.

The homogeneous Mathieu equation is given by,

$$\ddot{A}(\tau) + \mu\dot{A}(\tau) + [a + \epsilon + \epsilon\cos(\tau)]A(\tau) = 0. \tag{6}$$

The goal is to find periodic solutions to the Equation (6) using Lindstedt's perturbation method.[11] In this method, ϵ is assumed to be small and a solution to Equation (6) is sought in the form of the following expansion:

$$A(\tau) = A_o(\tau) + \epsilon A_1(\tau) + \epsilon^2 A_2(\tau) + \ldots \tag{7}$$

and

$$a = a_o + \epsilon a_1 + \epsilon^2 a_2 + \ldots \tag{8}$$

where $a_o, a_1, a_2 \ldots$ are constants. Since the periodic coefficients $\cos(\tau)$ in Equation (6) varies with a period of 2π, only two types of solutions exist - one with period 2π and the other with period 4π.[8] Hence, solutions involve functions $A_o(\tau), A_1(\tau)$, etc., which are either 2π or 4π periodic.

Substituting Equations (7) and (8) into Equation (6), allows one to collect terms in like powers of ϵ. Since $\epsilon \neq 0$, the coefficients to these terms must be zero. The first three of these coefficients (set to zero) are:

$$\ddot{A}_o(\tau) + a_o A_o(\tau) = 0 \tag{9a}$$

$$\ddot{A}_1(\tau) + a_o A_1(\tau) = -\hat{\mu}\dot{A}_o(\tau) - a_1 A_o(\tau) - A_o(\tau) - A_o\cos(\tau) \tag{9b}$$

$$\ddot{A}_2(\tau) + a_o A_2(\tau) = -\hat{\mu}\dot{A}_1(\tau) - a_2 A_o(\tau) - a_1 A_1(\tau) - A_1(\tau) - A_1\cos(\tau) \tag{9c}$$

The first order solution to these equations are

$$A_o(\tau) = \begin{cases} \cos(\sqrt{a_o}t) \\ \sin(\sqrt{a_o}t) \end{cases} = \begin{cases} \cos\left(\frac{n}{2}t\right) \\ \sin\left(\frac{n}{2}t\right) \end{cases}, \quad n = 0, 1, 2 \ldots \tag{10}$$

and $a_o = \frac{n^2}{4}, n = 0, 1, 2 \ldots$.

We now consider the specific values of n and solve the equations using the procedure given in reference.[11] At this point is also important to remember that one has to use the following approximation for $\hat{\mu} = \epsilon\mu$ for $n = 1$ and $\hat{\mu} = \epsilon^2\mu$ for $n = 2$ and so on for higher values of n. For this paper the highest order of ϵ that has been choose is $n = 2$. It is note worthy that solving the Equations (9a),(9b),(9c) gives the solutions for a in terms of the constants a_o, a_1 and a_2, and the modal amplitude $A(\tau)$ in terms of $A_o(\tau)$ and $A_1(\tau)$. These solutions are obtained by zeroing the coefficients of all terms on the right hand side of the Equation (9b),(9c), which render the solutions $(A_1(\tau), A_2(\tau))$ non periodic (secular).

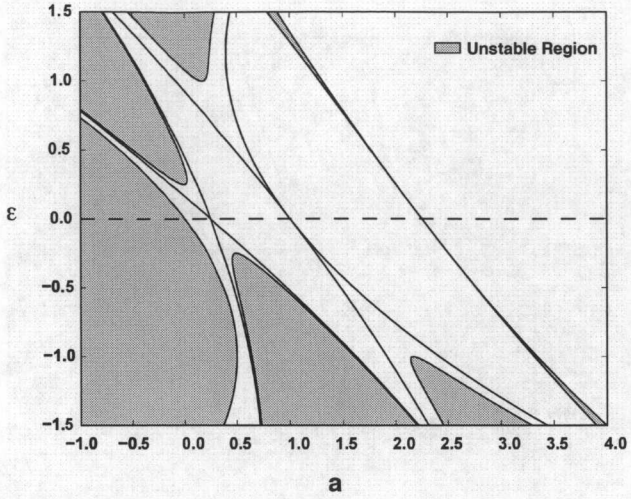

Figure 2: A parametric Mathieu stability diagram. This shows combinations of (a,ϵ) that lead to periodic behavior - separating stable and unstable regions. Two cases are shown: $\zeta = 0.0$ and 0.25

4. RESULTS

The objective is to plot parameter combinations that lead to periodic solutions (using the periodic solutions generated in section 3.2). These solutions neither grow nor decay and, hence, serve as a dividing line between asymptotically stable behavior and unstable behavior. To begin, the nondimensional parameters (ϵ, a) are considered, see Equation (6). These stability boundaries are then converted into physical meaningful parameters, namely the voltage squared and normalized excitation frequency.

4.1. Stability Behavior in Normalized Parameters: The (ϵ,a) Plane

The solution procedure described in section 3.2 rendered expressions for $a = a(\epsilon)$ for the cases $n = 0, 1, 2\ldots$ (see Equation (8)). These functions describe combinations of (a, ϵ) that lead to periodic solutions, indicating a stability boundary. These functions are explicity given by:

$$a = -\epsilon - \frac{\epsilon^2}{2} \tag{11}$$

$$a = \frac{1}{4} - \left(1 \pm \frac{1}{2\epsilon}\sqrt{\epsilon^2 - \mu^2}\right)\epsilon - \frac{\epsilon^2}{8}, \tag{12}$$

$$a = 1 - \epsilon + \left(\frac{1}{6} \pm \frac{1}{4\epsilon^2}\sqrt{\epsilon^4 - 16\mu^2}\right)\epsilon^2, \tag{13}$$

for the cases $n = 0, 1, 2$, respectively. These equations are plotted in Figure 2 for the cases $\zeta = 0, 0.25$. The leftmost curve corresponds to $n = 0$ and is independent of damping. The next two curves (from the left) that cross the $\epsilon = 0$ axis are related to the undamped $n = 1$ case. The damped $n = 1$ case is moved up off the axis and is rounded near the vertex. The unstable region is shaded and clearly indicates parameter combinations that lead to unbounded solutions. Additional cases are shown and progress to the right, as n increases. These curves are reminicent of those corresponding to the standard form of Mathieu's equation.[8, 11]

Points inside the shaded region denote unstable oscillations, which translates to large deformations and a high probability for the initiation of peeling (desticking the beam from the substrate). Obviously, as the structural damping is reduced, the unstable regions grow and (linearly) unbounded solutions are more likely. Of course, these parameter diagrams don't hold much insight into the physical parameters that will initiate debonding. Those are described in the following section.

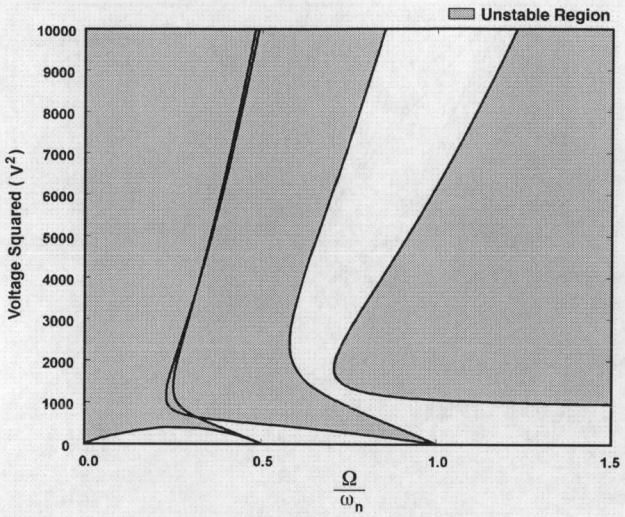

Figure 3: A stability plot in physical parameters: voltage squared vs. normalized frequency ($\zeta = 0.0$)

4.2. Stability Behavior in Physical Parameters: Voltage-Frequency Plane with $\zeta = 0$

While Figure (2) does contain all of the stability information for this system, the nature of the nomalization (which simplified the solution process) does not provide obvious insight into the physical parameters that lead to unstable oscillations. Hence, the stability curves given by Equations (11), (12), (13) may be re-expressed in terms of the excitation voltage and frequency using: $a = 1/4r^2$, $\epsilon = -\kappa a V_o^2$, and $\kappa = \epsilon_o \bar{A}/\delta^3 k$. For the undamped case presented in this section, closed form relations may be obtained for the square of the voltage as a function of the frequency ratio: $V_o^2 = V_o^2(r)$. The specific expressions are available in the thesis associated with this work.[9]

Figure (3) shows curves associated with periodic oscillations of this system with zero damping for the various cases $n = 0, 1, 2$. Again, the unstable zones, which promote stiction repair, are shaded. Interestingly, at low frequencies, the stable zones only exist for very low voltages. In fact, the unstable zones are quite large below $r = 0.5$; this is good news from a repair perspective. Above $r = 0.5$, larger stable zones emerge. At still higher frequencies ($r > 1.25$), the stable region exists at lower voltages and at extremely large voltages ($V_o^2 > 10000$). At intermediate voltages, this technique appears viable.

4.3. Stability Behavior in Physical Parameters: Voltage-Frequency Plane with $\zeta \neq 0$

Of course, real structures are damped. Moreover, there is considerable evidence in the literature that various forms of damping may contribute to the response of MEMS devices.[12–14] These include structural damping, squeeze-film damping, thermoplastic damping, etc. For simplicity, only structural (linear viscous) damping is considered. Several damping values are chosen based on the literature[12–14]: $\zeta = 0.0$, 0.25, 0.50, 0.75. In contrast to the undamped case, closed form relations for $V_o^2 = V_o^2(r)$ are not available in the undamped case. Instead, a line search approach had to be used. To begin, the expression $\epsilon = -\kappa a (V_o)^2$ is substituted into Equations (11), (12), and (13); this gives $a = a(V_o^2)$. The voltage is fixed at a value and the frequency (r) is incrementally swept from a low value to a high value. Knowing that $a = 1/4r^2$, this value of a is compared to $a = a(V_o^2)$. When these two values are equal, the resulting parameters (V_o, r) correspond to a periodic solution - denoting a stability boundary.

Figure 4 shows a stability plot of the voltage squared versus the normalized frequency for the four damping values given. The highlighted region shows the unstable zone for the most heavily damped case, $\zeta = 0.75$. As one might expect, as the damping increases, the stable zones are increased. This makes the repair procedure more challenging. However, it is worth noting that at higher frequencies, the unstable zone is uneffected by damping and, hence, may provide the best means for achieving a successful stiction repair.

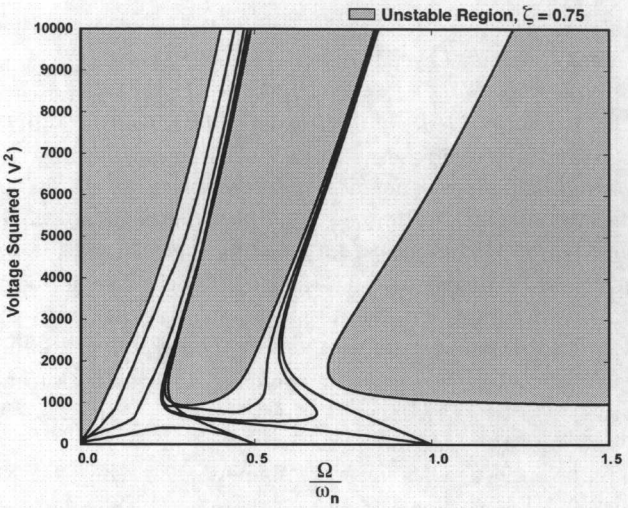

Figure 4: A stability plot in physical parameters: voltage squared vs. normalized frequency ($\zeta = 0.0, 0.25, 0.50, 0.75$)

5. CONCLUSIONS

This paper presents a new approach to stiction repair in MEMS devices. Specifically, it uses electrical actuation to promote (linearly) unstable oscillations in a stuck component. The idea is that these oscillations may grow sufficiently large so as to induce peeling of the component from a substrate, as shown in Figure (1). Using a perturbation stability analysis on the governing equation of motion, parameter combinations that lead to periodic oscillations are obtained. These parameters serve as stability boundaries in the parameter space. Moreover, the unstable zones have been clearly identified.

Because damping dramatically shrinks these unstable zones, the practical use of this approach becomes an issue. To make use of this method, it might be advantageous to sweep gradually through a variety of frequencies (for a given voltage); this significantly increases the likelihood that the system will fall into an unstable zone, such that the desired repair may be effected.

Finally, it should be pointed out that this repair technique has a hidden virtue. It may be combined with the resonance technique outlined for mechanical excitation.[7] Specifically, if the frequency sweep approach is taken, one may sweep in and out of unstable zones. However, in the stable zones the system may encounter a resonance, which could promote debonding. Repeated sweeps through unstable zones, coupled with resonances, would further increase the likelihood of success. Ultimately, experiments must be conducted to demonstrate the viability of this approach. Such experiments are already being developed by the authors.

Acknowledgments

The support of the National Science Foundation, Division of Civil and Mechanical Systems is gratefully acknowledged.

REFERENCES

1. N. Fujitsuka, and J. Sakata, "A New Processing Technique to Prevent Stiction Using Silicon Selective Etching for SOI-MEMS," *Sensors and Actuators A: Physical*, **97-98**, 716-719, 2002.
2. W.R. Ashurst, C. Yau, C. Carraro, C. Lee, G.J. Kluth, T.R. Howe, R. Maboudian, "Alkene Based Monolayer Films as Anti-Stiction Coatings for Polysilicon MEMS," *Sensors and Actuators A: Physical*, **91**(3), 239-248, 2001.

3. N. C. Tien, S. Jeong, L. M. Phinney, K. Fushinobu, J. Bokor, "Surface Adhesion Reduction in Silicon Microstructures Using Femotosecond Laser Pulses," *Applied Physics Letters*, **66**(2), 197-199, 1995.
4. K. Fushinobu, L. M. Phinney, and N. C. Tien, "Ultrashort-Pulse Laser Heating of Silicon to Reduce Microstructure Adhesion," *Internation Journal of Heat and Mass Transfer*, **39**(15), 3181-3186, 1996.
5. L. M. Phinney, J. W. Rogers, "Pulsed Laser Repair of Adhered Surface Micromachined Polycrystalline Silcon Cantilevers," *Journal of Adhesion Science and Technology*, **17**(4), 603-622, 2003.
6. J. W. Rogers, T. J. Mackin, and L. M. Phinney, "A Thermomechanical Model of Adhesion Reduction for MEMS Cantilevers," *Journal of Microelectromechnaical Systems.* **11**(5), 512-520, 2002.
7. A.A. Savkar, K.D. Murphy, M.R. Begley, and T. Mackin, "On the Use of Structural Dynamic Excitation to Release Stiction Failed MEMS," Manuscript in preparation.
8. N.W. McLachlan, *Theory and Application of Mathieu Functions,* Dover Publications, New York, 1964.
9. A.A. Savkar, *Vibration Repair of Micro-Scale Components,* Ph.D. Thesis, The University of Connecticut, 2005.
10. T. Mackin, *Personal Communication*, January, 2005.
11. A.H. Nayfeh, D.T. Mook, "Nonlinear Oscillations," John Wiley & Sons, Inc New York, 1995.
12. M. Bao, H. Yang, Y. Sun, Y. Wang, "Squeeze film air damping of thick hole plate," *Sensors and Actuators A Physical*, **108**, 212-217, 2003.
13. D. Homentcovschi, R.N. Miles,"Viscous damping of perforated planar micromechanical structures," *Sensor and Actuators A Physical*, **119**, 544-552, 2005.
14. A. Duwel, J. Gorman, M. Wienstein, J. Borenstein, P. Ward,"Experimental study of thermoelastic damping in MEMS gyros," *Sensor and Actuators A Physical*, **103**, 70-75, 2003.